A Modified Version of Canny Filter Applied to Identify Oxidation Points in Steel Plate

Antonio Eduardo Assis Amorim
College of Technology-JAHU (Fatec-JAHU)
Jahu, SP, Brazil

Líria Baptista de Rezende
College of Technology-JAHU (Fatec-JAHU)
Jahu, SP, Brazil

Suzana de Almeida Prado Pohl Sanzovo
College of Technology-JAHU (Fatec-JAHU)
Jahu, SP, Brazil

ABSTRACT
Steel plates are present in submerged vessels or civil structures and usually they are in aggressive environments which can initially cause an oxidation process leading to corrosion, which can compromise their physical integrity. Periodically they undergo surveys and depending on the depth or complexity of the structure, these operations are complex and costly. The use of cameras embedded in robotic vehicles allows the use of digital image processing techniques. Oxidation has a peculiar tint which allows the use of edge detection filters. Canny filter has two input parameters, standard deviation and the thresholds that affect the identification of the edges. The purpose in this study is to choose entropy and the threshold of the image and use them as input parameters in the Canny filter to identify the oxidation points. Two images are used, one of them of a piece in which the normalized histogram focuses on dark tones and the other that has a normalized histogram concentrated in light shades.

The parameter sigma is a polynomial function of entropy and threshold while the factor is an exponential function of entropy. It is analyzed the situation for both images, one is of a small piece of steel and the other one of a large piece of a ship in RGB and HSV components. Applied to both situations, it is observed that the code can identify the oxidation points of the plate in both light and dark normalized histograms. The results are promising, showing that the filter has a good behavior.

General Terms
Edge detection, Filter.

Keywords
Canny filter, Edge detection, Oxidation, Entropy, Image components.

1. INTRODUCTION
Ships operating in environments, whether at rivers or at sea, at the requirement of the Classification Society, insurance companies and the shipowner themselves, need periodically to carry out inspection to verify the integrity of the ship's structure and its equipment [1]. Fig. 1 shows a ship which under the action of time presents the deterioration of the paint on its hull.

The inspection involves a visual survey of the ship, as well as the testing the ship's systems and its structural elements. Some inspections require the removal of the vessel from the water and transporting it to a dry environment, a process known as docking, for inspection and maintenance [2]. These inspections are carried out over the vessel's lifetime, usually every five years, when its documentation expires.

Fig. 1: Oxidation on ships.

This process is a complex operation because it involves planning by the shipowner, the shipyard, and outsourced companies for hiring personnel and materials. The maneuver involves centering the ship over the drydock blocks, and also requires divers or submerged cameras [1]–[6].

Some of the inspections can be carried out with the vessel on water, if there have been no incidents which have compromised the structure, maneuvering and propulsion system of the vessel. In these cases, inspection can be done by divers or robotic vehicles with embedded camera.

The hull of the vessel is one of the parts involved in the inspection. It is the largest one and undergoes a visual inspection by the Classification Society in search of possible faults, either by agglomeration of barnacles, oxidation or corrosion points, or areas damaged by collisions.

The ship's hull features several areas exposed to oxidation and corrosion, ranging from the part which is always below the water line to splash zones that are just above the water line and the upper surfaces which can be damaged from water and weather [7].

The degradation of the steel plate begins with the oxidation process in the steel. If it is not treated, an electrified layer appears, and it leads to the corrosive process of the plate.

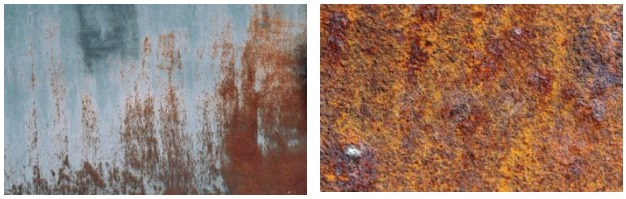

Fig. 2: Effects of oxidation. On the left side, oxidation forms a layer of electrical material with a characteristic color. On the right side, the advanced process of oxidation produces corrosion

As iron is one of the components of the steel, the tint of oxidation is very characteristic which allows the use of digital image processing to delineate or detect oxidized areas.

Detection and analysis can be performed by visual inspections, chemical or physical process [8].

Digital processing depends on the quality of images, being widely used because it is a nondestructive approach. Image quality affects the performance of the oxidation detection system on the plates [9]–[11]. The following factors may interfere with image processing:

- Lighting.
- Shadow.
- Noise.
- Surface discontinuities.
- Depth discontinuities.
- Color and texture discontinuities.
- Speculation.
- Reflectance.
- Light scattering.
- Turbidity.

It is considered that when analyzing a scene with a digital camera, part of the plate is oxidized or corroded. As there is an abrupt change in the shades of the image, they are treated as being an edge.

There is extensive literature which addresses the performance of these edge detection filters.

Details of these filters and their performances can be found at [12]–[19]. Some of these works analyze the performance of these filters for some types of images, whether binary (black and white) or grayscale. They basically identified that the edges produced by the Roberts, Sobel, Prewitt filters deviated slightly from the original image. And similar results were also observed when analyzing other filters [20].

In another analysis the authors noted that Sobel, Prewitt, Robert filters are inaccurate, while the Canny filter had better accuracy when compared to other filters [9]. The Canny filter can detect false "zero crossing", whereas the LoG filter can detect the edges in various directions, being noise sensitive.

Some approaches involve the modifying of the filters. One of them is to adapt the Kirsch filter in order to obtain good results from the edges [21].

Most of these filters have parameters that can be adjusted. In this way, it is possible to connect these parameters to other indicators that can be extracted from the original image, such as the thresholds, normalized histogram of the image or its entropy.

In this approach there is a work which observed the behavior of these filters in grayscale images, in terms of image entropy. The analysis is done in terms of the Peak Signal-to-Noise Ratio - PSNR and average quadratic error - MSE. The results showed that the Canny Filter reaches the highest entropy value and the lowest PSNR values, showing that it is an adequate filter for the detection of edges [10].

Using two parameters coupled in each of the Sobel filter components, there is an improvement in image contrast [22]. In another study, the entropy behavior of the image of oxidized steel plates over the course of a week is analyzed. The results showed that the Canny filter is suitable for identifying the oxidation areas [23].

The proposal of this article involves the analysis of two images which contain areas degraded by oxidation, one of them is a small piece of a steel plate and the other one is a piece of a ship structure.

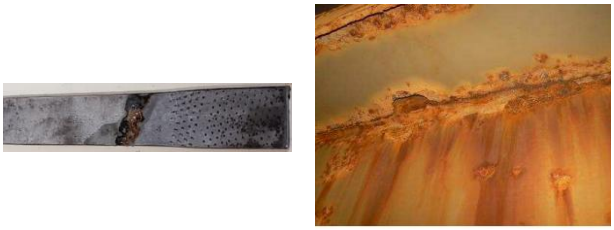

Fig. 3: The picture on the left side shows a small piece of steel; the one and on the right, the part of a ship

For the first image, the normalized histogram focuses on dark tones while the second image has a normalized histogram concentrated in light shades.

The RGB components, in grayscale and HSV components are extracted from the image. In each of the components, it is obtained the normalized histogram, entropy, and thresholds. The entropy and thresholds are used as input parameters of the Canny filter.

The code is written in Octave. A comparison of the results are done with usual the Canny filter.

2. CODE

The code written in Octave has the following structure, as shown in Fig. 4.

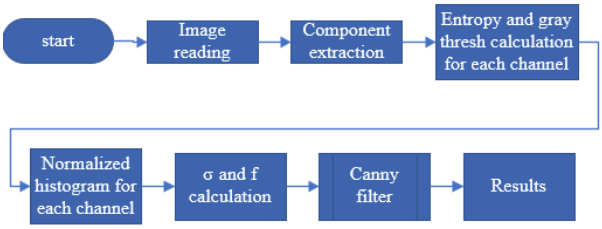

Fig. 4: Code flowchart

The first steps of the code involve reading the image file, extracting the RGB components, grayscale, and HSV. For each component entropy and thresholds are calculated, the image on each component is presented as well as its normalized histogram.

The Canny filter has two parameters, the standard deviation of the filter σ and the thresholds f.

These parameters are used in the Canny filter as follows

$$\sigma = g^s, \quad (1)$$

and

$$f = g(1 - e^s). \quad (2)$$

The Canny thresholds are calculated by using the expressions

$$\begin{aligned} T_{low} &= \sigma/10 \\ T_{high} &= f/4 \end{aligned} \quad (3)$$

3. RESULTS

Fig. 5 shows the first image in RGB and grayscale components. Visually there is no difference between the images.

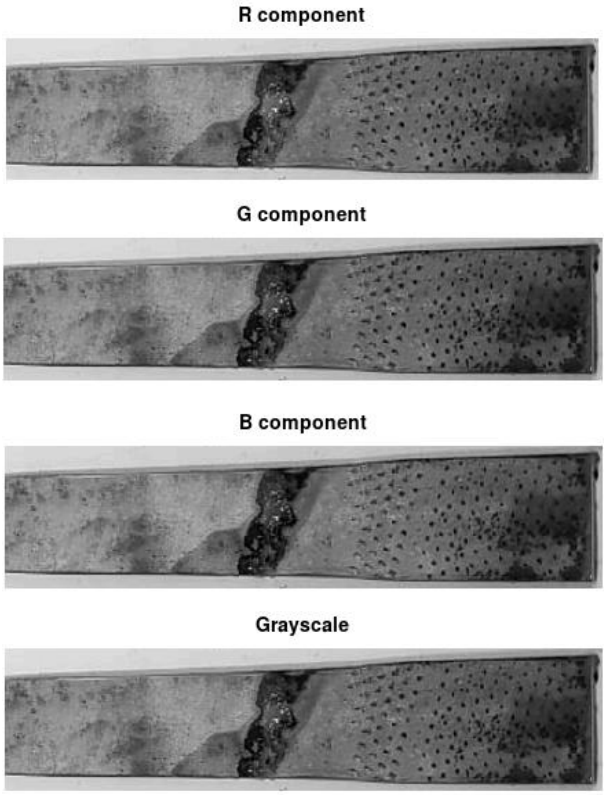

Fig. 5:Image of the small piece in RGB and grayscale components

Fig. 6 shows the normalized histogram of the small piece in RGB and grayscale components. It is observed that the histograms are similar, with peaks in 100 and 200. No matter the choice of the component, RGB or grayscale, the results will be similar.

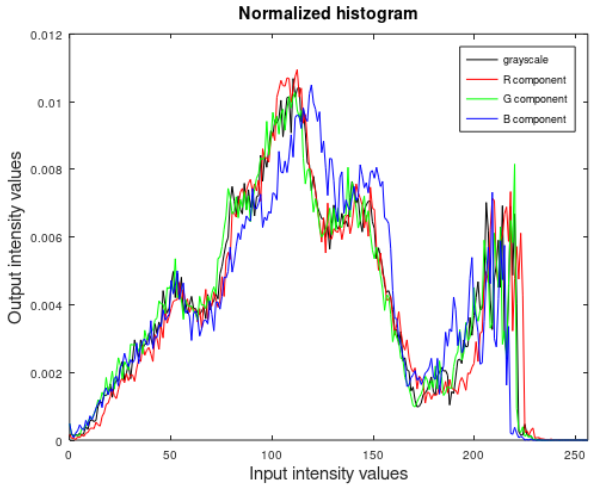

Fig. 6: Normalized histogram in RGB and grayscale components

Table 1 shows the entropy values in each of the components, indicating very similar results in all of them. In the same way, when analyzing the thresholds in each of the components, there is also a slight variation, being larger in component R and smaller in component B.

Table 1: Values of entropy in each of the components for the small piece

Indicator	R	G	B	Grayscale
Entropy	7,5021	7,5298	7,5130	7,5196
Thresholds	0,5137	0,4863	0,4627	0,4941

The results are quite different when are analyzed in HSV components, as shown in Fig. 7. Note that the H and S components apparently highlight the oxidized part.

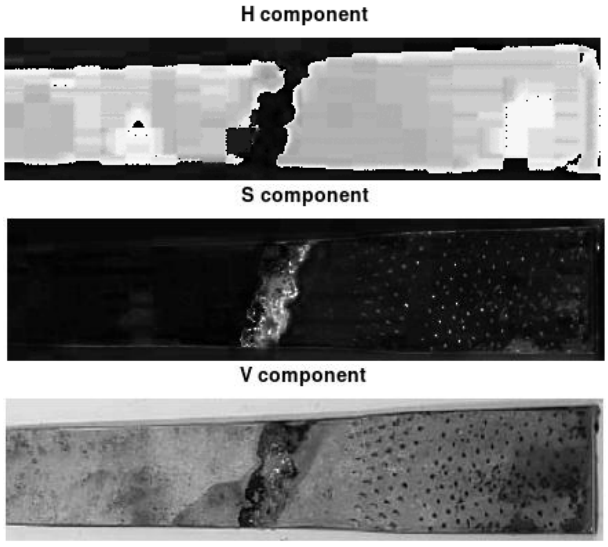

Fig. 7: Image in HSV component.

Fig. 8 shows the normalized histogram on each of the HSV components. Note that the H component focuses on the ends, with peaks around 25 and peaks in the range of 175 to 250. The S component shows peaks around 25 while the V component is distributed along the values, with very small values of intensity.

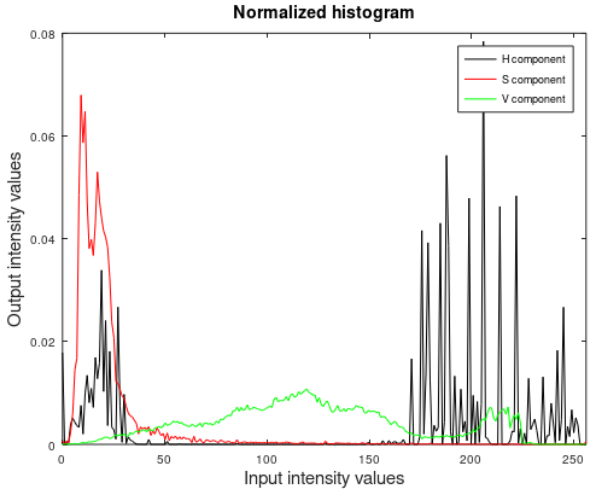

Fig. 8: Normalized histogram in HSV components.

In Table 2, it is shown the entropy and gray thresholds values in each of the HSV components. Note that entropy is higher in component V. When analyzing the gray thresholds in each of the components, the values vary, being larger in component V and smaller in component S, providing a different result from the previous image.

Table 2: Entropy and gray thresholds values in the HSV component.

Indicator	H	S	V
Entropy	5,6136	5,2270	7,5082
Threshold	0,4569	0,2431	0,5137

Fig.9 shows the results of the processed images. It is observed that the encoding identifies the oxidized parts, and the choice of the component yields similar results.

Now, it is analyzedthe image of a piece of a ship. Fig. 10 shows the image in RGB and grayscale components of an oxidized part of the ship and the histogram in Fig. 11.

Visually, the R component is lighter while component B is darker. The G component and grayscale are apparently similar. The results are quite different when it is analyzed this issue with a small piece. The histograms are quite different. As visually noted, the R component peak is at 200 while component B peak is at 50. The peak in the G component and the grayscale component are similar.

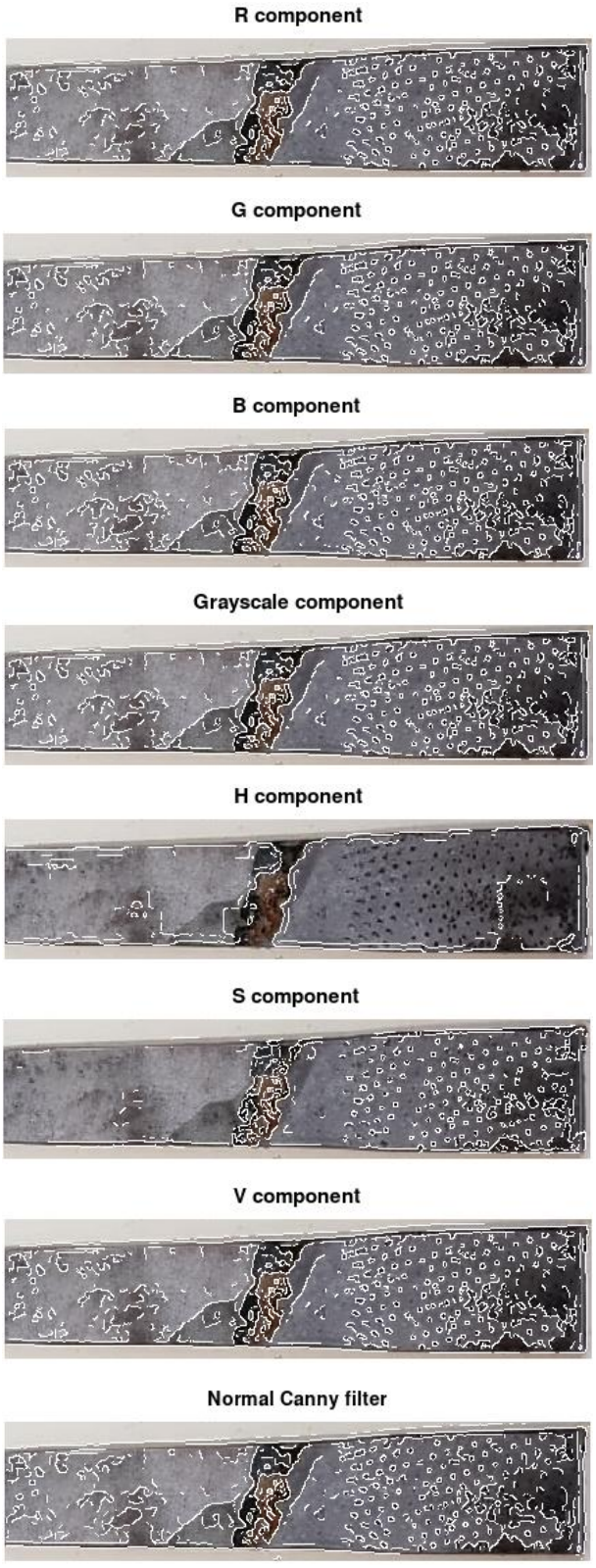

Fig. 9: Processed image in the respective components.

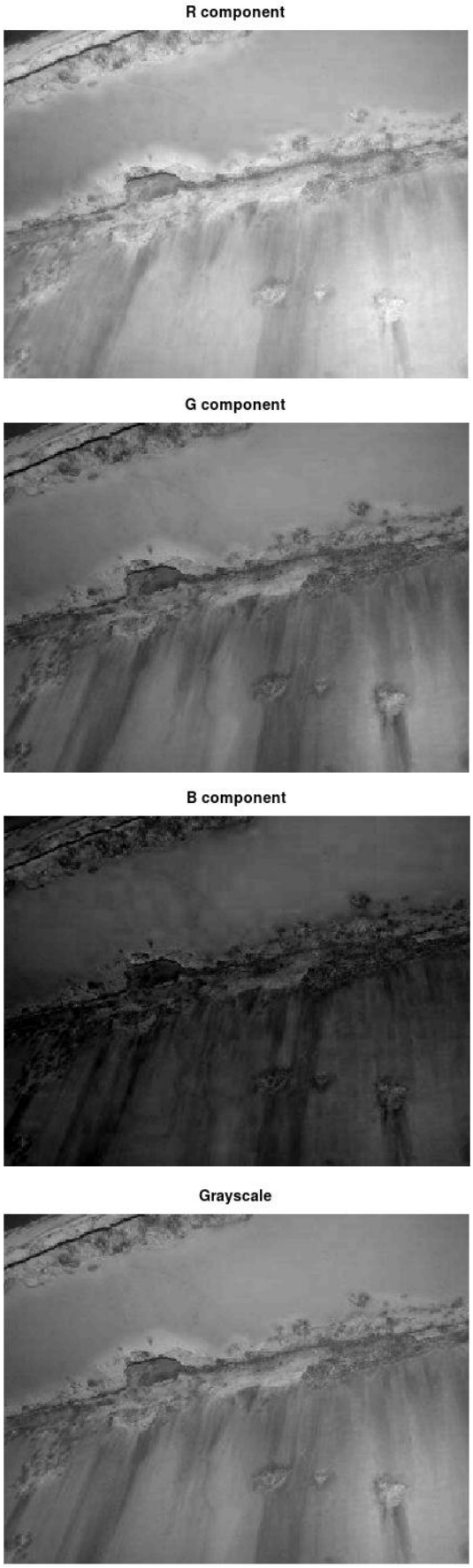

Fig. 10: Image of a large piece in RGB and grayscale components.

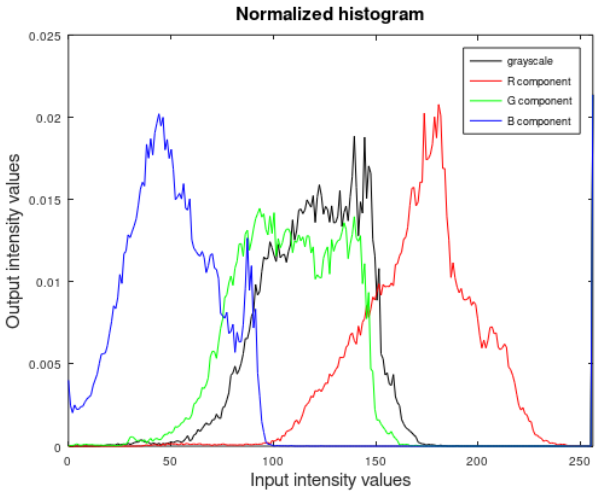

Fig. 11: Normalized histogram for a large piece.

Table 3 shows the entropy values in each of the components. Note that they vary in each of the components, being larger on component R and smaller on component B. On the other hand, when analyzing the threshold in each of the components, they vary, being larger in component B and smaller in component G.

Table 3: Entropy values in each of the components.

Indicator	R component	G component	B component	Grayscale
Entropy	6,7347	6,5981	6,3912	6,5103
Threshold	0,6588	0,4431	0,7392	0,4824

Moreover, the problem of oxidation can be analyzed by looking at HSV components, as shown in Fig. 12. H component is darker while S component is brighter. The image of the V component is like the ones of RGB and grayscale components.

Note that when the image is of a small part, the H or S component already shows the oxidation edges. However, when it is considered the image of a larger piece, the results in HSV components are different. Therefore, it is inconclusive to say which component is the best component to do the analysis.

Fig. 13 shows the normalized histogram for HSV components. Note that the H component peaks around 25 while both the S component and the V component peak at 200.

In contrast to the image of a small piece, the normalized histogram of the larger part shows a different distribution, that is, the way the photo is taken interferes with the results.

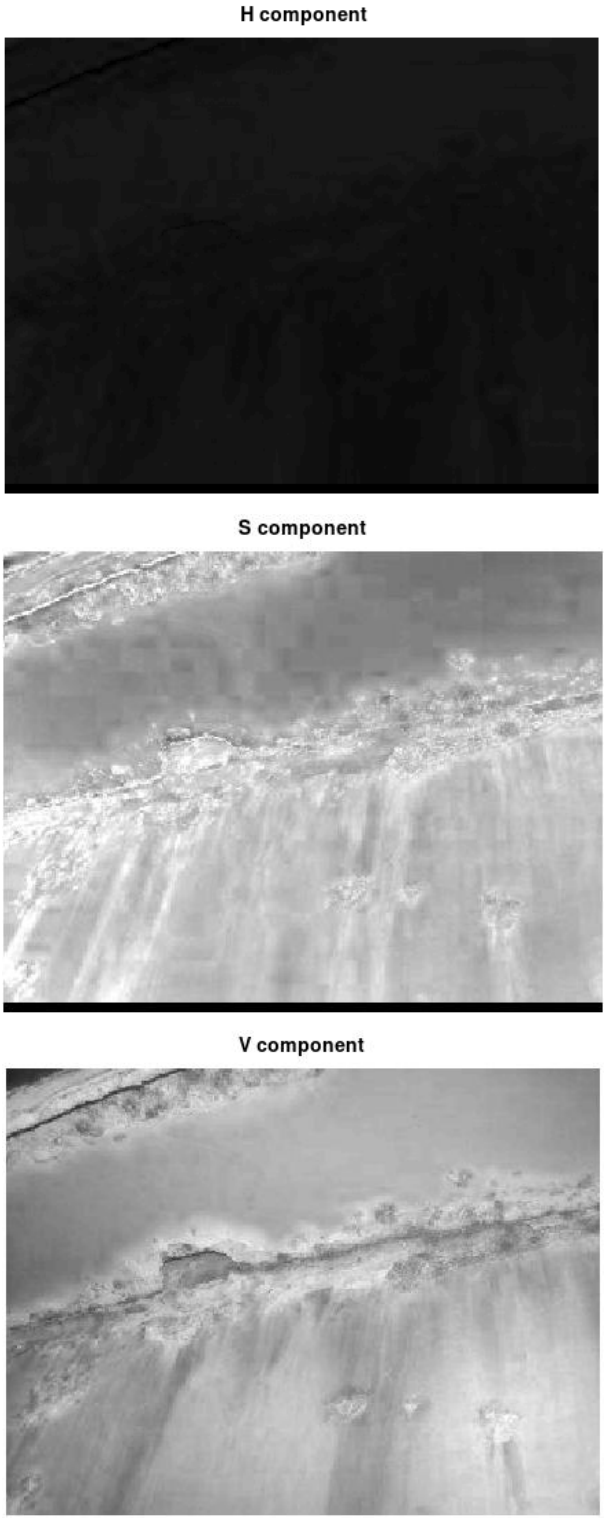

Fig. 12: HSV components for a large piece

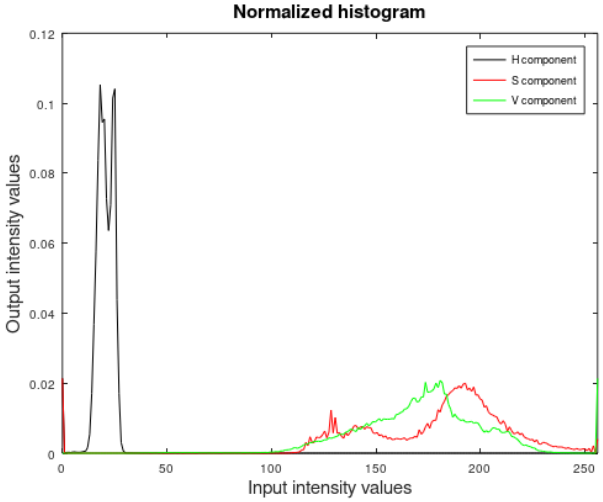

Fig. 13: Normalized histogram of HSV components for a large piece

4. CONCLUSION

In this paper, two images are analyzed containing oxidized parts. The first image refers to a small plate whereas the second one to a structural part of a ship.

In **Table 4Error! Reference source not found.** the values for entropy and threshold values in each of the HSV components are shown. Note that entropy is higher in components S and V. When analyzing threshold, components S and V have the highest values while the H component has a lower value.

Table 4. Entropy and threshold values for HSV components

Indicator	H component	S component	V component
Entropy	3,8185	6,7866	6,7347
Threshold	0,074510	0,6353	0,6588

Fig. 14 shows the results of applying the Canny filter to identify the oxidation points in components RGB and grayscale. Fig. 15 shows the results for components HSV. The R, G and V and grayscale components present equivalent results in the identification of points with oxidation. Components B and S show few stretches of oxidation while the H component shows excessive marks.

The code extracts the components RGB, grayscale and HSV from these images, the thresholds, and the entropies. These two pieces of information were used as input for the Canny filter to detect the oxidized regions on the steel plate.

The code was written using the Octave and the results are compared with the usual command for edge detection for the Canny filter.

For the first image, which corresponds to a small piece of steel, it is observed that images in which the normalized histograms are similar, the choice of the component is not relevant. The results of edge detection for RGB and V components are quite equivalent to the Canny filter. Only for H and S components the results are different given that the values for entropy also are different.

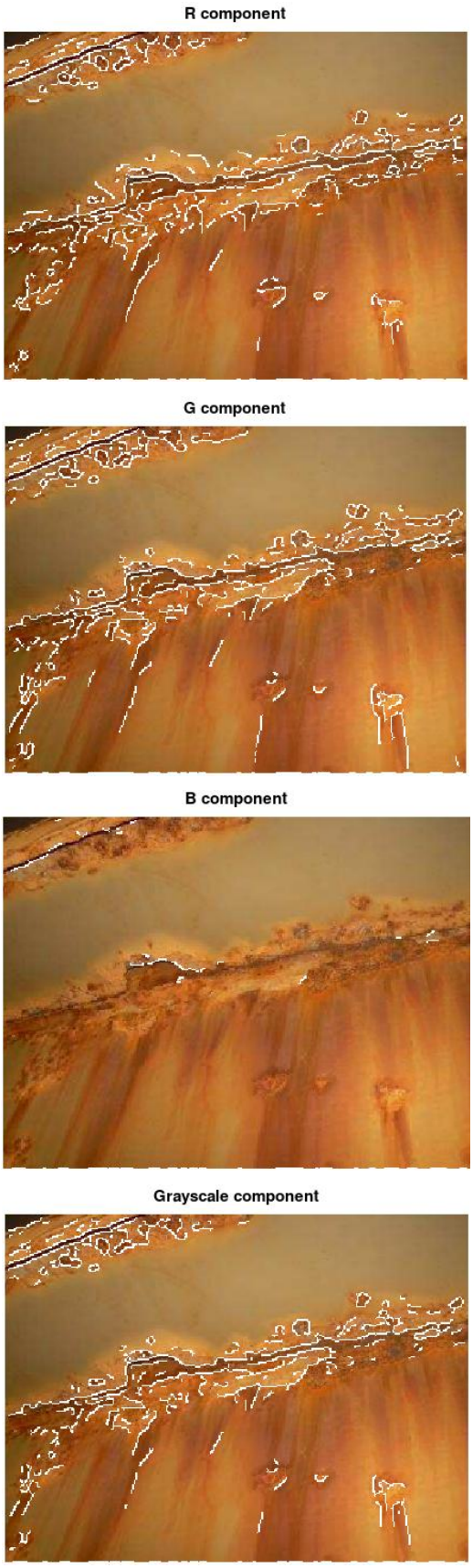

Fig. 14: Processed image in RGB components and grayscale showing the oxidation points

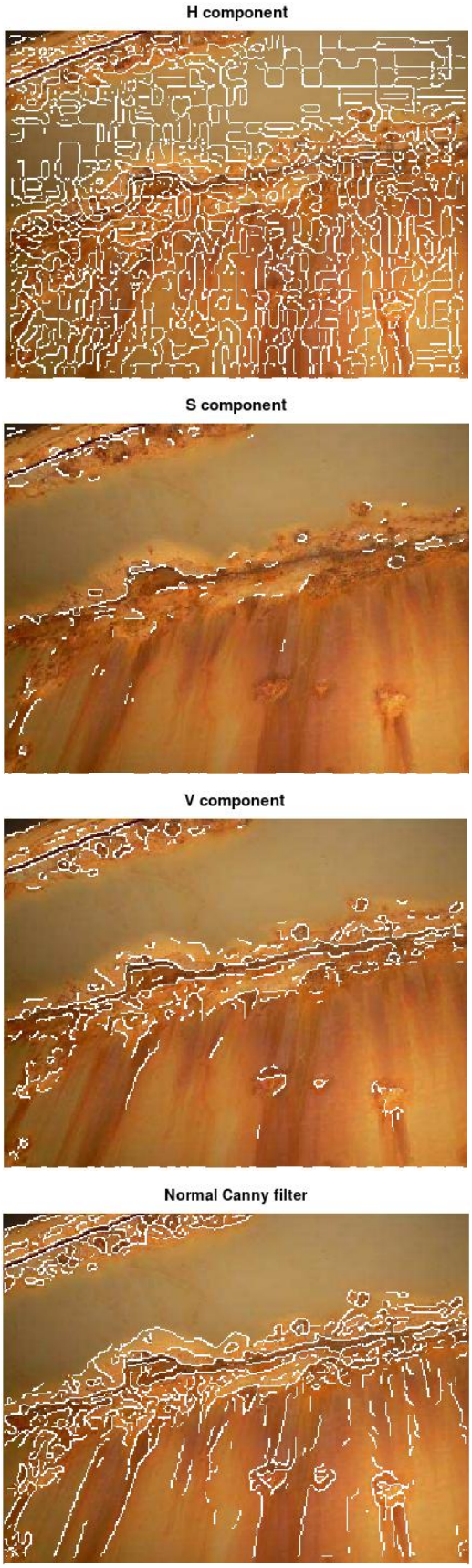

Fig. 15: Processed image in HSV components and with normal Canny filter showing the oxidation points

For the second image, which corresponds to a piece of a structure of a ship, only the G component and grayscale histograms are equivalent. However, the values for entropy are very similar while the thresholds are different. The results show that there is a small attenuation to detect edges in R, G and gray component. For the B component there is a little edge detection. The S and V histograms are equivalent like the values for entropy and threshold. However, the results for edge detection are very different. The worst result is for the H component.

As a conclusion, it isexpected that these results can shed some light on improvements for the implementation of the mathematical model for detection of oxidation points in steel plates.

5. REFERENCES

[1] E. J. C. Neves, "Docagem de embarcações – navios graneleiros," UFRJ, 2019.

[2] J. E. Modica, "Riscos em Projetos de Docagem de Navios Petroleiros," USP, 2009.

[3] L. A. Demsetz and J. Cabrera, "Detection Probability Assessment for Visual Inspection of Ships," 1999.

[4] C. Fernández-Isla, P. J. Navarro, and P. M. Alcover, "Automated Visual Inspection of Ship Hull Surfaces Using the Wavelet Transform," Math. Probl. Eng., vol. 1, pp. 1–12, 2013.

[5] J. R. de Souza, "Gestão De Projeto Para Docagem De Navios Em Diques," Universidade Cândido Mendes, 2010.

[6] J. M. dos S. S. Rodrigues, "Simulador Interactivo de Docagem de Navios em Ambiente Tridimensional," Instituto Técnico de Lisboa, 2008.

[7] T. F. da Rocha, "Medidas de proteção à corrosão em cascos de navios militares brasileiros," Universidade Cândido Mendes, 2011.

[8] S. Kumar Ahuja, "Surface Corrosion Detection and Classification for Steel Alloy using Image Processing and Machine Learning," Helix, vol. 8, no. 5, pp. 3822–3827, 2018.

[9] J. S. Owotogbe, T. S. Ibiyemi, and B. A. Adu, "Edge Detection Techniques on Digital Images - A Review," Int. J. Innov. Sci. Res. Technol., vol. 4, no. 11, pp. 329–332, 2019.

[10] P. P. Acharjya, R. Das, and D. Ghoshal, "Study and Comparison of Different Edge Detectors for Image Segmentation," Glob. J. Comput. Sci. Technol., vol. 12, no. 13, 2012.

[11] P. H. Buscariolloand A. E. A. Amorim, "Avaliação do desempenho de um sistema de visãoaplicadoaoveículosubmersívelnãotripuladoJaú II," Fatecnológica, vol. 5, p. 9, 2010.

[12] R. C. Gonzalez and R. E. Woods, Digital Image Processing. Pearson Education - Prentice Hall, 2018.

[13] O. Marques, Practical Image and Video Processing Using MATLAB. Hoboken, New Jersey: John Wiley & Sons, 2011.

[14] S. Gupta, C. Gupta, and S. K. Chakarvarti, "Image Edge Detection: A Review," Int. J. Adv. Res. Comput. Eng. Technol., vol. 2, no. 7, pp. 2246–2251, 2013.

[15] A. Çelik et al., "Signal Processing, Image Processing, and Pattern Recognition," in International Conference, SIP 2009, 2009, vol. 1, no. 1, p. 341.

[16] G. N. Manjula and M. Ahmed, "A Survey on Various Methods of Edge Detection," J. Sci. Technol., vol. 1, no. 1, pp. 25–28, 2016.

[17] S. Vijayarani and A. Sakila, "A Performance Comparison of Edge Detection Techniques for Printed and Handwritten Document Images," Int. J. Innov. Res. Comput. Commun. Eng., vol. 4, no. 5, pp. 8327–8337, 2016.

[18] M. Juneja and P. S. Sandhu, "Performance Evaluation of Edge Detection Techniques for Images in Spatial Domain," Int. J. Comput. Theory Eng., vol. 1, no. 5, pp. 614–621, 2009.

[19] C. Ghosh, S. Majumder, S. Ray, S. Datta, and S. N. Mandal, "Different EDGE Detection Techniques: A Review," in Lecture Notes in Electrical Engineering, vol. 686, no. November, 2020, pp. 885–898.

[20] A. Maan and D. S. Singh, "A Review Paper on Image Segmentation Using Edge Detection Techniques and Threshold in MATLAB," J. Netw. Commun. Emerg. Technol., vol. 7, no. 6, pp. 30–33, 2017.

[21] J. S. Y. Sia, T. S. Tan, A. Bin Yahya, M. F. T. Tiong, and J. Y. X. Sia, "Mini Kirsch Edge Detection and Its Sharpening Effect," Indones. J. Electr. Eng. Informatics, vol. 9, no. 1, pp. 228–244, Mar. 2021.

[22] A. E. A. Amorim and M. J. P. Cacchi, "Digital Image Processing for Recognition of Imperfections in the Submerged Hull," Int. J. Innov. Sci. Res. Technol., vol. 5, no. 2, pp. 765–767, 2020.

[23] A. E. A. Amorim and M. J. P. Cacchi, "Evaluation of Edge Detection Filters Applied to Corroded Steel Sheets," Int. J. Innov. Sci. Res. Technol., vol. 5, no. 6, pp. 898–902, 2020.